

Static and electrochemical performance of ecofriendly extract as antiscalant and corrosion inhibitor in desalination plants

R.H. Khaled^a, A.M. Abdel-Gaber^{a,b,*}, H.T. Rahal^a, R. Awad^c

^aDepartment of Chemistry, Faculty of Science, Beirut Arab University, Lebanon, emails: ashrafmoustafa@yahoo.com (A.M. Abdel-Gaber), rimaa_k@hotmail.com (R.H. Khaled), hananrahal88@yahoo.com/hrahal@bau.edu.lb (H.T. Rahal)

^bDepartment of Chemistry, Faculty of Science, Alexandria University, Ibrahimia, P.O. Box: 426, Alexandria 21321, Egypt

^cDepartment of Physics, Faculty of Science, Beirut Arab University, Lebanon, email: ramadan.awad@bau.edu.lb

Received 27 April 2019; Accepted 25 October 2019

ABSTRACT

The impact of *Ceratonia siliqua* L. (carob) leaf extract as an antiscalant in an alkaline CaCl₂ brine solution was examined using the static anti-scaling technique, conductivity, and chronoamperometry measurements as well as optical photographic study. Mineral scales were deposited from the brine solution by cathodic polarization of the mild steel surface to -0.8 V. The electrochemical behavior of the formed film was tested in simulating seawater solutions (0.5 M NaCl) using electrochemical impedance spectroscopy (EIS) technique. Functional groups and organic compounds of carob leaf extract were identified by Fourier transform infrared spectroscopy and gas chromatography-mass spectroscopy. The obtained results showed that carob leaf extract can be used safely as an antiscalant and corrosion inhibitor for cooling systems. Moreover, the used techniques showed that scale deposits and the surface area occupied decreased with increasing carob leaf extracts concentrations. EIS measurements revealed that carob leaf extract retards the corrosion rate of steel in simulating seawater solutions.

Keywords: Carob; Mild steel; Green inhibitors; Anti-scalant; Chronoamperometry; Scales

1. Introduction

Scale formation is a serious issue often seen in several areas including heat exchangers, cooling towers, water transport, distillation, and oil or gas production [1–4]. Such scale deposits cause pipes clogging which in turn diminishes heat transfer efficiency, leading sometimes to plant shutdown and accordingly to severe economic losses [2–5]. The nonproductive expenses related to scale were estimated to be about 0.8, 3.0, and 9.0 billion dollars in Great Britain, Japan, and the USA [6]. Therefore, it is crucial to understand scale formation, to know the types of scale, as well as to control the scaling process in cooling water systems because it may have a positive impact on the development of new

high-performance materials and on the evolution of effective anti-scaling methods.

Calcium carbonate (CaCO₃) is the most abundant constituent of scales deposited from natural water. It exists in three types depending on the crystal structure: vaterite (spherical), aragonite (needle-shaped) and calcite (cubic) [7]. The Inhibition mechanism of scale deposits can range from basic dilution methods to the most advanced threshold scale inhibitors. Most of these chemicals block the growth of the scale particles by hindering the growth of scale nuclei. A few chemicals chelate or tie up the reactant in soluble form. Because chelating agent consumes scale ions in stoichiometric ratios, the effectiveness of chelates as scale inhibitors are poor. In contrast, threshold scale inhibitors interact chemically with crystal nucleation sites and considerably

* Corresponding author.

reduce crystal growth rates [8]. They inhibit the formation of mineral scale approximately 1,000 times than a balanced stoichiometric ratio [9]. There are thousands of chemicals used as scale inhibitors for diverse applications [10–17]. Nowadays, increasing environmental concerns and discharge limitations have imposed additional challenges in scale hindering processes. This has prompted researchers to test plant extracts as environmentally friendly antiscalant for CaCO₃ calcareous deposits on mild steel in cooling water systems [2–4,18–23].

A first strategy developed by Abdel-Gaber et al. [2] was to consider extracts from trees with large economic benefits, which grow well under calcareous soil conditions in the Mediterranean coastal zone as antiscalants. Indeed, these trees have a strong ability to accumulate calcium, which constitutes a high percentage of the mineral mass in the aboveground parts of these trees. Abdel-Gaber et al. [2–4] reported inhibition of CaCO₃ scale performed with fig leaf extract. Moreover, they used olive leaf extract and tested its scale inhibition [2].

The carob tree (*Ceratonia siliqua* L.) is a tree native to the Mediterranean region. It was known by ancient Greeks, who carried it to Greece and Italy [24]. Carob cultivation in marginal and usual calcareous soils of the Mediterranean region is vital environmentally and economically [24].

The present work investigates the influence of carob leaf extract as a green inhibitor for the formation of calcium carbonate calcareous deposits on mild steel in an alkaline CaCl₂ brine solution. As well, it explores the electrochemical corrosion behavior of the film formed in simulating seawater solutions.

2. Experimental studies

2.1. Solution preparation

Distilled water and analytical reagent-grade ethylenediaminetetraacetic acid (EDTA), NaCl, NaHCO₃, Na₂SO₄ and CaCl₂ were purchased from Sigma-Aldrich, (St. Louis, Missouri, United States). The composition of the CaCl₂ brine solution was 0.7 M NaCl, 0.0025 M NaHCO₃, 0.028 M Na₂SO₄ and 0.01 M CaCl₂ [2].

2.2. Extraction procedure

Carob stock solution was prepared in the same manner as reported previously [25,26]. Carob leaves were dried for 2 h in an oven at 80°C and ground to powder form. A weight of 10 g sample of the powder was refluxed in 100 mL distilled water for 1 h. The refluxed solution was filtered to remove any contamination. The concentration of the stock solution was determined by evaporating 10 mL of the filtrates and weighing the residue. The concentration of the stock solution was expressed in terms of part per million (ppm).

2.3. Fourier transform infrared spectroscopy and gas chromatography-mass spectroscopy analysis

Fourier transform infrared spectroscopy (FTIR) analysis of the carob extract was carried by FTIR 8400S Shimadzu, (Kyoto, Japan) in the spectral region between 400 and 4,000 cm⁻¹. Gas chromatography-mass spectroscopy

(GC-MS) analysis of the carob leaf extract was performed using Shimadzu QP 2010, (Shimadzu Europa GmbH, Duisburg) plus with series gas chromatography coupled with Shimadzu QP 2010 plus mass spectroscopy detector (GC-MS) system.

2.4. Static anti-scaling experiment

The anti-scaling activity was examined by static scale inhibition experiment according to GB/T 16632-2008 [10,27–29]. In this experiment, 500 mg CaCl₂ was mixed with 500 mg NaHCO₃ in 1 L distilled water to ensure that $\rho_{(Ca^{2+})} = \rho_{(HCO_3^-)} = 500 \text{ mg L}^{-1}$ (as CaCO₃). The pH of the resultant mixture was adjusted to 9.1 with a borax buffer solution (Na₂[B₄O₅(OH)₄]·8H₂O). Then, the mixture was distributed into different volumetric flasks, where different concentrations of carob leaf extract (25, 50, 100, 200, 500, and 600 ppm) were added to each flask and incubated at 80°C for 14 h. The free Ca²⁺ was titrated with 0.01 mol L⁻¹ EDTA. The anti-scaling efficiency (η) was calculated according to the equation:

$$\eta = \frac{\rho_2 - \rho_1}{\rho_0 - \rho_1} \times 100$$

where ρ_2 was mass concentration of Ca²⁺ with inhibitor after heating for 14 h; ρ_0 and ρ_1 were mass concentration of Ca²⁺ without inhibitor before and after heating for 14 h, respectively.

2.5. Conductivity test

The conductivity of the solution is measured during titration with 0.1 M Na₂CO₃ using a conductivity meter. Prior to each experiment, 5 mL of 0.1 M CaCl₂ solution is added to an appropriate volume of the stock solution of carob leaf extract; then the mixture is completed to 100 mL with distilled water. Na₂CO₃ titrating solution was added in portions of 0.1 mL each.

2.6. Electrochemical studies

Chronoamperometry and electrochemical impedance spectroscopy (EIS) measurements were done using frequency response analyzer (FRA)/potentiostat supplied from ACM Instruments (UK). The measurements were carried out as reported in the previous study [30–33] in an electrochemical cell of three-electrode mode; platinum wire and saturated calomel electrodes (SCE) were used as counter and reference electrodes. The mild steel used for constructing the working electrode was of the following chemical composition (wt.%) (C: 0.271, Mn: 0.610, Si: 0.141, S: 0.034, P: <0.005, and Fe: 97.80). The steel rod of cylindrical shape was encapsulated in Teflon in such a way that only one surface was left uncovered. The exposed area (0.7853 cm²) was mechanically abraded with a series of emery papers of variable grades, starting with a coarse one and proceeding in steps to the finest (800) grade. Chronoamperometry tests were done by polarizing the steel electrode to -0.8 V (vs. SCE) in the test solution for 180 min. EIS measurements were performed at rest potential in 0.5 M NaCl solution just after the scale deposition process. The frequency range

for EIS measurements was 96×10^4 Hz to 0.1 Hz with an applied potential signal amplitude of 10 mV. Prior to EIS measurements, the working electrode was left to attain the open circuit potential in the test solution. All the measurements were done at $30^\circ\text{C} \pm 0.1^\circ\text{C}$ using the WiseCircu water bath (Germany) in solutions open to the atmosphere under unstirred conditions.

2.7. Optical micrographic study

Optical Photographs were taken with a 12-megapixel Canon camera that is linked to a personal laptop.

3. Results and discussion

3.1. GC-MS and FTIR analysis

The GC-MS chromatogram of the major compounds detected in carob leaf extract is shown in Fig. 1. The active compounds with their retention time are displayed in Table 1. Fifteen compounds were identified in carob leaf extract. The results revealed that 5,5-Dimethyl-2(5H)-furanone, loliolide (two isomers), n-hentriacontanol-1, 3-methylbut-3-en-2-one as well as long-chain alcohols are present as one of the major components in the carob leaf extract. Most of these compounds can be used as a promising natural replacement of antimicrobial chemicals for food safety and preservation as well as antibacterial, antioxidants, and anti-proliferative chemicals towards hepatocellular carcinoma cells, colon cancer cells, and the gastrointestinal tract [34,35]. The results of FTIR analysis presented in Fig. 2 confirmed the presence of alcohols, ketones, aromatic ring as well as alkanes are in accordance with the results obtained from GC-MS analysis. It could be concluded from matching the data obtained from GC-MS and FTIR that the active chemical ingredients may be 3,5-dihydroxy-6-methyl-2,3-dihydro-4h-pyran-4-one, syringaldehyde and (-)loliolide.

3.2. Antiscalant behavior of carob leaf extract

It must be noted that the conductivity and the static anti-scaling methods are screening assessments, similar to that provided by The National Association of Corrosion Engineers standards [36] that indicate the ability of the carob leaf extract to hinder the precipitation of calcium carbonate from the solution [2–4]. These test methods describe the tendency of carob leaf extract to inhibit scale in the solution (complex forming, dispersion, and liquefaction) and are not applicable to film-forming inhibitors.

3.2.1. Static anti-scaling data

Fig. 3 shows the variation of anti-scaling efficiency of carob leaf extract obtained from static measurements. The plot is characterized by an initial rising part followed by a saturated constant part at higher carob leaf extract concentrations. It is observed that the efficiency increased from 19.1% up to 80.8% for 600 ppm carob. Thus, the carob leaf extract has a promising anti-scaling effect against CaCO_3 scale deposits in cooling water systems.

3.2.2. Conductivity measurements

The variation of conductivity of CaCl_2 solution containing 400 ppm carob leaf extract with the amount of ml added of sodium carbonate is presented in Fig. 4. The variation grows linearly straight with increasing the added volume of Na_2CO_3 up to a point where the solution became turbid and supersaturated. This observation revealed fast precipitation of CaCO_3 followed by a drop in the conductivity. Subsequently, additional Na_2CO_3 after complete precipitation yields more ions in the solution leading to an increase in conductivity again.

The variation of supersaturation volume, which is the volume after which precipitation of added Na_2CO_3 occurs, as a function of carob leaf extract concentration (Fig. 5) shows

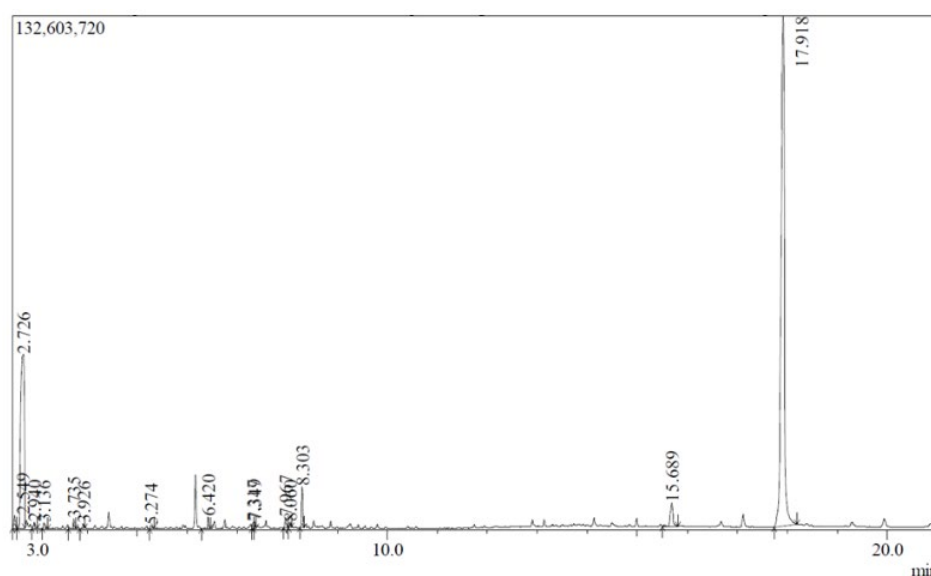
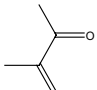
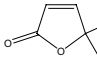
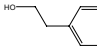
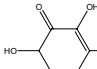
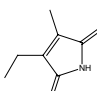
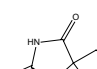
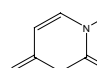
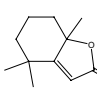
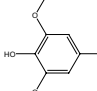
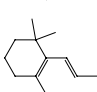
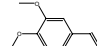
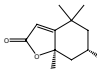
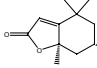



Fig. 1. Typical chromatogram of the compounds present in carob leaf extract.

Table 1
GC-MS chromatogram of carob leaf extract

| Retention time | Name of detected compounds | Structure | Formula | Molecular weight (g mol ⁻¹) | Peak area % | Activity |
|----------------|--|---|---|---|-------------|---|
| 2.549 | 3-methylbut-3-en-2-one |  | C ₅ H ₈ O | 82.12 | 0.81 | Used as fragrance and plant and animal metabolite |
| 2.726 | 5,5-dimethyl-2(5H)-furanone |  | C ₆ H ₈ O ₂ | 112.13 | 24.00 | Used as a key flavoring compound |
| 2.940 | beta.-phenylethyl alcohol |  | C ₈ H ₁₀ O | 122.16 | 0.37 | Used as flavor and fragrance |
| 3.136 | 3,5-dihydroxy-6-methyl-2,3-dihydro-4h-pyran-4-one |  | C ₆ H ₈ O ₄ | 144.12 | 0.30 | Antimicrobial, anti-inflammatory and antioxidant |
| 3.735 | Methylethylmaleimide |  | C ₇ H ₉ NO ₂ | 139.15 | 0.48 | Anti-oxidant |
| 3.926 | gamma.-methyl.-gamma.-ethylsuccinimide |  | C ₇ H ₁₁ NO ₂ | 141.17 | 0.27 | Anticonvulsant |
| 5.274 | 1-methyl-2,4(1H,3H)-pyrimidinedione |  | C ₅ H ₆ N ₂ O ₂ | 126.11 | 0.19 | Metabolite |
| 6.420 | 2(4H)-benzofuranone, 5,6,7,7a-tetrahydro-4,4,7a-trimethyl- |  | C ₁₁ H ₁₆ O ₂ | 180.24 | 0.59 | Fragrance |
| 7.317 | Syringaldehyde |  | C ₉ H ₁₀ O ₄ | 182.17 | 0.34 | Hypoglycemic agent and a plant metabolite |
| 7.349 | beta.-ionol |  | C ₁₃ H ₂₂ O | 194.31 | 0.30 | Flavor and fragrance agent |
| 7.967 | gamma.-hydroxy isoeugenol |  | C ₁₀ H ₁₂ O ₃ | 180.2 | 0.55 | No activity reported |
| 8.060 | (-)-loliolide |  | C ₁₁ H ₁₆ O ₃ | 196.24 | 0.24 | Medicine for nervous system |
| 8.303 | (-)-loliolide |  | C ₁₁ H ₁₆ O ₃ | 196.24 | 1.96 | Medicine for nervous system |
| 15.689 | n-hentriacontanol-1 |  | C ₃₁ H ₆₄ O | 452.8 | 2.25 | Traditional medicine and experimental therapy |
| 17.918 | Long chain alcohol | R-OH (R = long chain) | ROH | – | 67.37 | – |

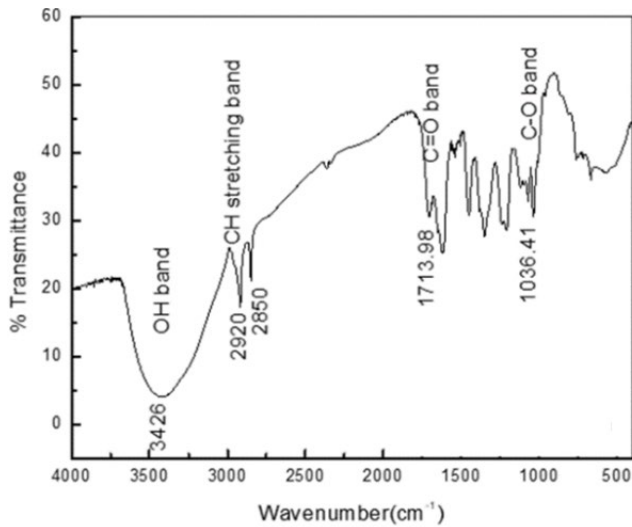


Fig. 2. FTIR spectra of carob plant leaf extract.

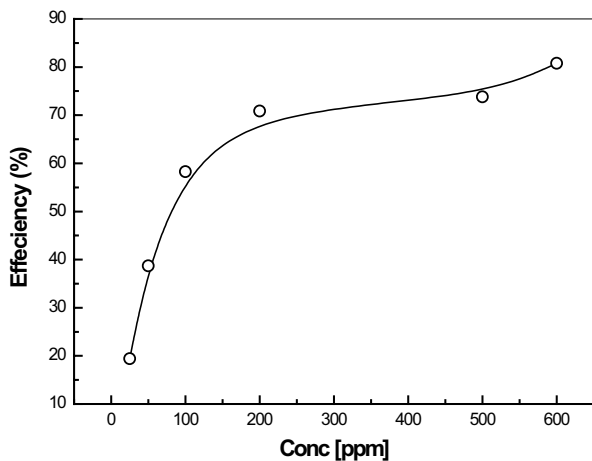


Fig. 3. Variation of the anti-scaling efficiency against CaCO_3 as function of the different concentrations of carob leaf extract (25, 50, 100, 200, 500, and 600 ppm).

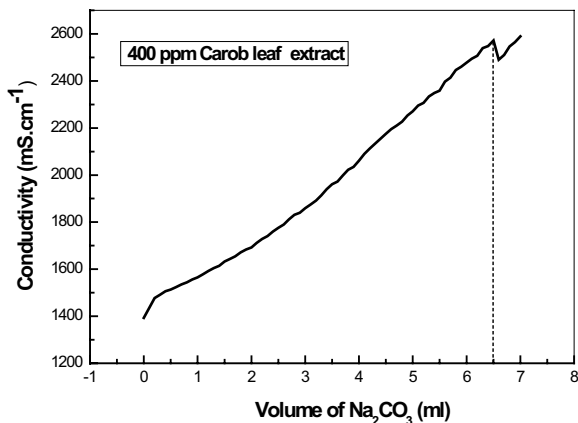


Fig. 4. Variation of solution conductivity of CaCl_2 containing 400 ppm carob leaf extract with the amount of sodium carbonate added.

that the supersaturation volume increases with increasing carob leaf extract concentration. This reveals that the extract hinders the supersaturation that may be credited to the adsorption of the extract molecules onto the active sites of the growing crystals leading to the liquefaction of suspended solids and thus reducing the rate of crystal growth [2]. Hence, these screening tests clarify that the carob leaf extract could be classified as an eco-friendly anti-scalant in an alkaline CaCl_2 brine solution.

3.2.3. Chronoamperometry measurements and optical micrographic study

Fig. 6 shows the chronoamperometric current-time experiments carried out at -800 mV vs. SCE for the polarized mild steel electrode in CaCl_2 brine solution in the absence and presence of different carob leaf extract concentrations

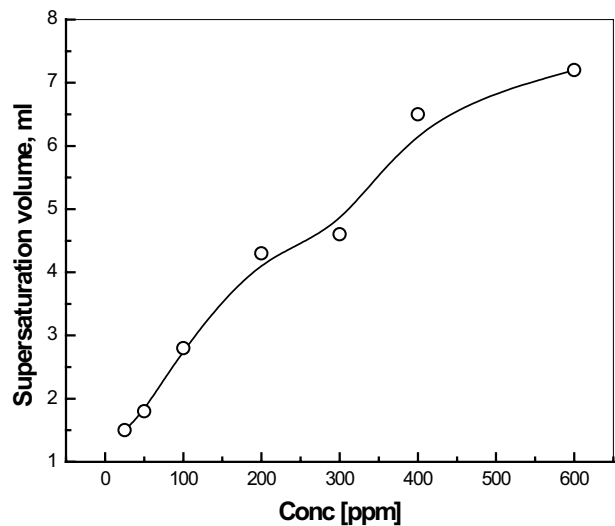


Fig. 5. Variation of supersaturation volume of Na_2CO_3 as a function of carob leaf extract concentration.

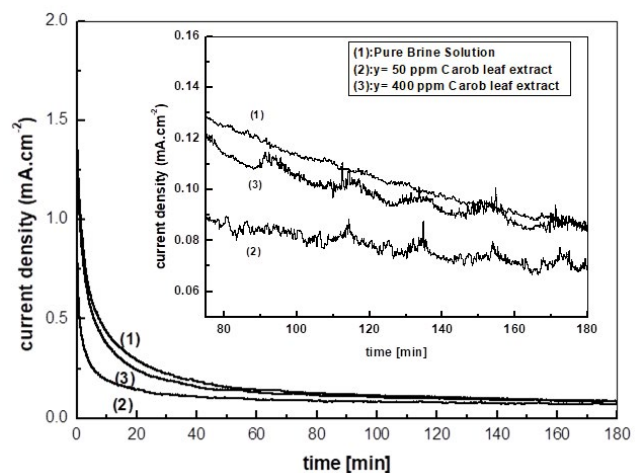


Fig. 6. Chronoamperometry curves for polarized mild steel electrode in the CaCl_2 brine solution in the absence and presence of different carob leaf extract.

(50 and 400 ppm) for 180 min. It is reported that the scales grow on metal surfaces under cathodic polarization [2]. These scales shield the active surface area accessible for the electrochemical reactions and accordingly reduce the corrosion current (i_{corr}) values [18,19]. As seen, two distinct regions appeared in Fig. The first is the crystal growth and the second which is the surface coverage, however, the stage of nucleation is not observed. The current decreased sharply with time until it reaches a steady-state value. The linear decrease of current revealed the deposition of CaCO_3 scales on the mild steel surface [3]. The inset of Fig. 6 shows a zoomed-in view of the chronoamperometric current variations between the tested solutions. The final values of the resulting current did not reach zero suggesting that the scale is porous and did not form a blocked film.

Fig. 7 shows the variation of current density obtained from chronoamperometry curves for polarized mild steel electrode in the CaCl_2 brine solution as a function of carob leaf extract concentrations at different intervals. Fig. 7 indicates that the minimum current densities were obtained at 180 min suggesting complete surface coverage by scale or adsorbed film of the molecules extracted from leaf extract. It is generally known that the low carbon steel microstructure consists of pearlite and ferrite. The pearlite itself consists of bands (or lamellar structure) of ferrite and cementite. Dugstad et al. [37] stated that both lab experiments and field experience have shown that the protective properties and the adherence of the film can vary greatly for carbon steels with apparently the same composition and microstructure. There is, however, no agreement about the mechanism and how microstructure affects the growth and stability of the formed film. Figs. 8a–f shows the optical micrographic photos obtained after 180 min of polarizing steel in CaCl_2 brine solution as a function of carob leaf extract concentration. In our previous study, the microscopic micrograph photos for the formation of calcareous deposits under cathodic polarization in CaCl_2 brine solution display that, in the absence

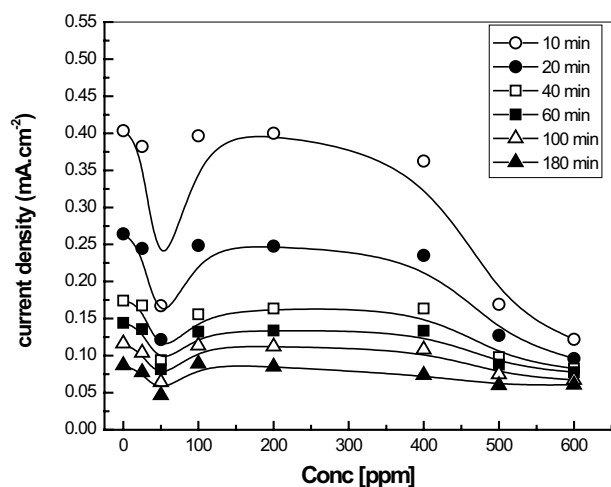


Fig. 7. Variation of the current density (i_{chrono}) obtained from the analysis of chronoamperometry curves at different time intervals for polarized mild steel as a function of carob leaf extract concentration.

of the antiscalant, a complete surface coverage takes place by extremely dense scale of distorted calcite crystals takes place [3]. Figs. 7 and 8a–f display that the higher current density was obtained in the absence of carob leaf extract indicating that the surface is covered by a porous scale film. From 25–50 ppm carob, the current decreased due to the adsorption of the carob extract molecules over the porous scale film filling up its voids as shown in Figs. 8b and c [38]. On increasing the carob leaf extract concentration to 200 ppm, the chronoamperometric current increased. Such behavior may be due to the adsorption of the carob extract molecules over the calcium carbonate particles leading to a partial liquefaction of scale film or interfere of the molecules with the crystal growth and formation processes [39]. From 200–600 ppm, the resultant current decreases indicating that the extract not only impedes the scale formation but also adsorbs on the mild steel surface forming an adsorbed film. The thickness of the adsorbed film increases with increasing the extract concentration, Figs. 8e and f. The optical micrographic photos confirm the dual mechanism for scale inhibition. Some extracted chemicals act as chemicals chelate that tie up the reactant in soluble form. On the other hand, other chemicals act threshold scale inhibitors interact chemically with crystal nucleation sites and considerably reduce crystal growth rates.

The obtained results are in quite good agreement with those obtained earlier from conductivity and static measurements. All techniques approve the ability of carob leaf extract to act as anti-scalant for CaCO_3 calcareous deposits.

3.3. Electrochemical behavior of the formed film in the presence of carob leaf extract

3.3.1. Electrochemical impedance measurements

Figs. 9a and b show the fitted Nyquist and Bode plots of mild steel that was cathodically polarized in a brine solution in the presence of 50 ppm carob leaf extract in 0.5 M NaCl. The Nyquist plot consists of two overlapped semicircles followed by a diffusion tail. The first semi-circle is clearly

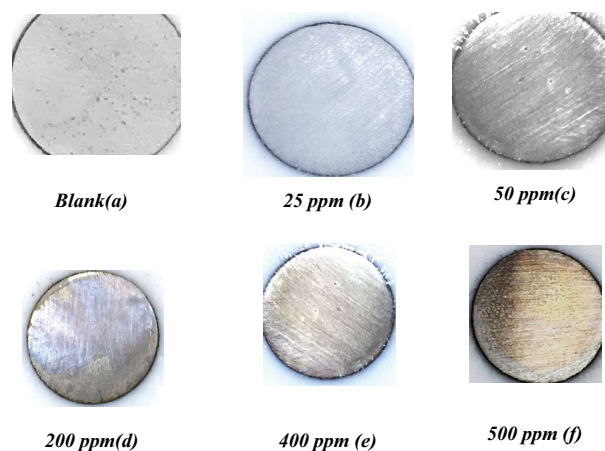


Fig. 8. (a–f) Optical micrographic photos obtained after 180 min of polarizing steel in CaCl_2 brine solution as a function of carob leaf extract concentration.

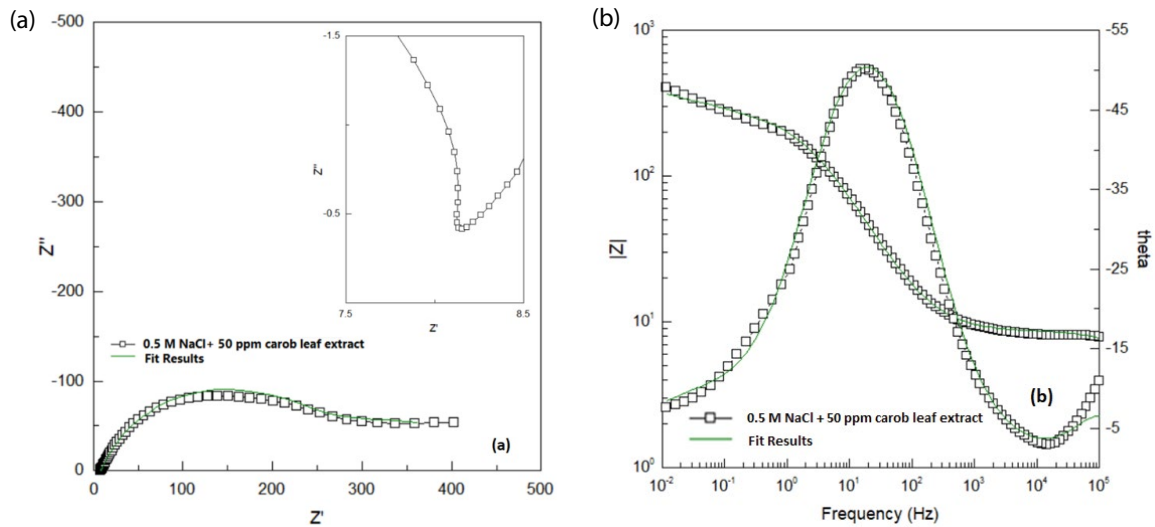


Fig. 9. Fitted Nyquist (a) and Bode (b) plots of mild steel, that was cathodically polarized in a brine solution in the presence of 50 ppm carob leaf extract, in 0.5 M NaCl.

shown in the zoomed inset of the figure. The value of the phase angle is lesser than 90 in Bode theta plot depicted in 9b, suggesting the presence of non-ideal capacitance that approves the inhomogeneities in the system [2,40]. The observed angle near 45° signifies fast ion diffusion in the electrolyte and adsorption onto the electrode surface and recommends the ideally pure capacitive behavior of the mild steel electrode [39].

The fitting of the spectrum to the equivalent circuit model permits the evolution of the elements of the circuit analog. Fig. 10 shows the equivalent circuit model used to analyze the impedance plots for mild steel in 0.5 M NaCl solutions. The circuit consists of R_s , the solution resistance, R_f is resistance associated with the layer of scale deposits formed during polarizing mild steel in brine solution and C is the corresponding film ideal capacitance. The R_{ct} denotes the charge transfer resistance and constant phase element (CPE₁) is the CPE₁ corresponding to double-layer capacitance. The CPE₁ is defined by two values, the non-ideal double-layer capacitance (Q_{dl}) and a constant (n). For a non-homogeneous system, n values range from 0.9 to 1. R and CPE₂ are the resistance and the constant phase element corresponding to the diffusion term, respectively.

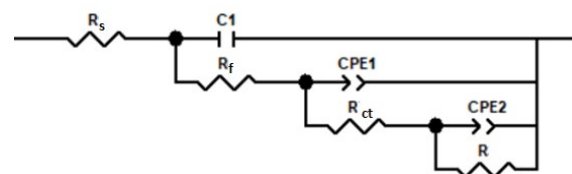


Fig. 10. Equivalent circuit model.

The values of electrochemical impedance parameters with the inhibition efficiency (%P) obtained from fitting the experimental data to the used equivalent model are presented in Table 2.

Inspection of the tabulated data clarifies that increasing the carob leaf extract concentrations up to 50 ppm increases the charge transfer resistance accompanied by a reduction in the non-ideal film capacitance. Such behavior can be attributed to the reduction of surface porosity and the adsorption of the extract molecules on the scale film which in turn delays the diffusion of the electrolyte to the metal surface and increase the charge transfer resistance [19]. However, increasing the extract concentration to 200 ppm decreases R_{ct} values explaining the liquefaction and removal of the scale

Table 2

Electrochemical impedance parameters of mild steel, which was cathodically polarized in a brine solution in the presence and absence of different leaf extract concentration, in 0.5 M NaCl

| Conc. (ppm) | R_s (ohm cm ²) | C_{dl} (F cm ⁻²) | R_{film} (ohm cm ²) | R_{ct} (ohm cm ²) | Q_1 (μF cm ⁻²) | n_1 | Q_2 (μF cm ⁻²) | n_2 | R (ohm cm ²) |
|-------------|------------------------------|--------------------------------|-----------------------------------|---------------------------------|------------------------------|-------|------------------------------|-------|----------------------------|
| Blank | 6.5 | 7.09×10^{-7} | 2.60 | 186 | 1,280 | 0.60 | 20,000 | 0.63 | 99 |
| 25 | 7.3 | 1.46×10^{-6} | 1.73 | 224 | 630 | 0.74 | 15,300 | 0.42 | 100 |
| 50 | 6.9 | 9×10^{-7} | 1.74 | 249 | 570 | 0.75 | 16,500 | 0.50 | 220 |
| 200 | 5.5 | 5.95×10^{-7} | 2.59 | 103 | 700 | 0.70 | 10,100 | 0.41 | 245 |
| 400 | 6.0 | 4.02×10^{-7} | 2.50 | 212 | 680 | 0.76 | 16,400 | 0.51 | 205 |
| 500 | 5.8 | 5.37×10^{-7} | 2.15 | 241 | 960 | 0.72 | 18,100 | 0.59 | 513 |

deposit by the leaf extracts as shown in Fig. 8d. This behavior proves that the extract acts as an antiscalant. Increasing leaf extracts concentrations above 200 ppm lead to an increase in the charge transfer resistance. This indicates that the extract does not only hinder deposits formation but also adsorbs on the mild steel surface creating a protective barrier for the dissolution of mild steel in a brine solution. The thickness of the adsorbed film increases with increasing carob leaf extract concentration.

Based on Fig. 8c and Table 2, to be cost-effective it is recommended to use 50 ppm of carob leaf extract since it gives an acceptable percent of corrosion inhibition (25%) and a good antiscalant behavior.

4. Conclusion

Carob leaf extract acted as both an environmentally friendly scale and corrosion inhibitor retarding the rate of scale formation in brine solutions and the corrosion of mild steel. The results suggested that some extracted chemicals act as chemical chelates and others as threshold scale inhibitors. A good agreement between the scale inhibition efficiencies calculated by different static and electrochemical techniques was attained. The obtained results indicated that carob leaf extract could be applied safely as an antiscalant and corrosion inhibitor in different cooling systems

References

- [1] T. Rabizadeh, D.J. Morgan, C.L. Peacock, L.G. Benning, Effectiveness of green additives vs. poly (acrylic acid) in inhibiting calcium sulfate dihydrate crystallization, *Ind. Eng. Chem. Res.*, 58 (2019) 1561–1569.
- [2] A.M. Abdel-Gaber, B.A. Abd-El-Nabey, E. Khamis, D.E. Abd-El-Khalek, Investigation of fig leaf extract as a novel environmentally friendly antiscalant for CaCO₃ calcareous deposits, *Desalination*, 230 (2008) 314–328.
- [3] A.M. Abdel-Gaber, B.A. Abd-El-Nabey, E. Khamis, H. Abd-El-Rhmann, H. Aglan, A. Ludwick, Green antiscalant for cooling water systems, *Int. J. Electrochem. Sci.*, 7 (2012) 11930–11940.
- [4] A.M. Abdel-Gaber, B.A. Abd-El-Nabey, E. Khamis, D.E. Abd-El-Khalek, A natural extract as scale and corrosion inhibitor for steel surface in brine solution, *Desalination*, 278 (2011) 337–342.
- [5] A. Neville, T. Hodgkiess, A.P. Morizot, Electrochemical assessment of calcium carbonate deposition using a rotating disc electrode (RDE), *J. Appl. Electrochem.*, 29 (1999) 455–462.
- [6] J. Li, M. Tang, Z. Ye, L. Chen, Y. Zhou, Scale formation and control in oil and gas fields: a review, *J. Dispersion Sci. Technol.*, 38 (2017) 661–670.
- [7] D. Peronno, H. Cheap-Charpentier, O. Horner, H. Perrot, Study of the inhibition effect of two polymers on calcium carbonate formation by fast controlled precipitation method and quartz crystal microbalance, *J. Water Process Eng.*, 7 (2015) 11–20.
- [8] M. Crabtree, D. Eslinger, P. Flecher, M. Miller, A. Johnson, G. King, Fighting scale-removal and prevention, *Oilfield Rev.*, 11 (1999) 30–45.
- [9] L. Rosenstein, Process of Treating Water, US Patent No. 2,038,316, April 21, 1936.
- [10] H.Y. Li, W. Ma, L. Wang, R. Liu, L.S. Wei, Q. Wang, Inhibition of calcium and magnesium-containing scale by a new antiscalant polymer in laboratory tests and a field trial, *Desalination*, 196 (2006) 237–247.
- [11] D.E. Abd-El-Khalek, B.A. Abd-El-Nabey, Evaluation of sodium hexametaphosphate as scale and corrosion inhibitor in cooling water using electrochemical techniques, *Desalination*, 311 (2013) 227–233.
- [12] C.X. Liu, Y.J. Liu, Y.H. Zhou, Y.Y. Liao, Development of research on scale inhibitor in land, *Hebei Chem. Eng. Ind.*, 32 (2009) 15–17.
- [13] S. Tadier, S. Rokidi, C. Rey, C. Combes, P.G. Koutsoukos, Crystal growth of aragonite in the presence of phosphate, *J. Cryst. Growth*, 458 (2017) 44–52.
- [14] R. Ketrane, B. Saidani, O. Gil, L. Leleyter, F. Baraud, Efficiency of five scale inhibitors on calcium carbonate precipitation from hard water: effect of temperature and concentration, *Desalination*, 249 (2009) 1397–1404.
- [15] X. Yang, G. Xu, The influence of xanthan on the crystallization of calcium carbonate, *J. Cryst. Growth*, 314 (2011) 231–238.
- [16] M. Chaussemier, E. Pourmohtasham, D. Gelus, N. Pécou, H. Perrot, J. Lédion, O. Horner, State of art of natural inhibitors of calcium carbonate scaling. A review article, *Desalination*, 356 (2015) 47–55.
- [17] W. Zhang, G. Li, F. Jin, Y. Huo, T. Sun, C. Li, Synthesis and characterization of an ionic liquid-carboxylic acid copolymer scale inhibitor and its scale inhibition performance, *Water Sci. Technol. Water Supply*, 19 (2019) 1463–1472.
- [18] E. Khamis, E. El-Rafey, A.M. Abdel-Gaber, A. El-Hefnawy, M.S. El-Din, Arghel Extract as an Environmentally Friendly Anti-Corrosion and Anti-Scaling in Industrial Water Systems, *IOP Conference Series: Materials Science and Engineering*, Vol. 301, IOP Publishing-Bristol, England, 2018.
- [19] E. Khamis, E. El-Rafey, A.M. Abdel-Gaber, A. Hefnawy, N. Galal El-Din Shams El-Din, M. Salah El-Din Esmail Ahmed, Comparative study between green and red algae in the control of corrosion and deposition of scale in water systems, *Desal. Wat. Treat.*, 57 (2016) 23571–23588.
- [20] O. Horner, H. Cheap-Charpentier, X. Cachet, H. Perrot, J. Lédion, D. Gelus, F. Roussi, Antiscalant properties of *Herniaria glabra* aqueous solution, *Desalination*, 409 (2017) 157–162.
- [21] Z. Belarbi, J. Gamby, L. Makhlofi, B. Sotta, B. Tribollet, Inhibition of calcium carbonate precipitation by aqueous extract of *Paronychia argentea*, *J. Cryst. Growth*, 386 (2014) 208–214.
- [22] D. Hasson, H. Shemer, A. Sher, State of the art of friendly “green” scale control inhibitors: a review article, *Ind. Eng. Chem. Res.*, 50 (2011) 7601–7607.
- [23] B.A. Miksic, M.A. Kharshan, A.Y. Furman, Vapor Corrosion and Scale Inhibitors Formulated From Biodegradable and Renewable Raw Materials, *European Symposium on Corrosion Inhibitors*, Ferrara-Italy, 2005.
- [24] I. Battle, J. Tous, Carob Tree: *Ceratonia Siliqua* L.-Promoting the Conservation and Use of Underutilized and Neglected Crops. 17, Bioersivity International, 1997.
- [25] R.S. Al-Moghrabi, A.M. Abdel-Gaber, H.T. Rahal, A comparative study on the inhibitive effect of *Crataegus oxyacantha* and *Prunus avium* plant leaf extracts on the corrosion of mild steel in hydrochloric acid solution, *Int. J. Ind. Chem.*, 9 (2018) 255–263.
- [26] R.S. Al-Moghrabi, A.M. Abdel-Gaber, H.T. Rahal, Corrosion inhibition of mild steel in hydrochloric and nitric acid solutions using willow leaf extract, *Prot. Met. Phys. Chem.*, 55 (2019) 603–607.
- [27] L. Yuan, C. Zou, C. Li, L. Lin, W. Chen, Evaluation of β -cyclodextrin-polyethylene glycol as green scale inhibitors for produced-water in shale gas well, *Desalination*, 377 (2016) 28–33.
- [28] J. Chen, H. Xu, J. Han, C. Wang, Q. Wu, C. Li, A green multifunctional antiscaling inhibitor for crystallization control of Ca-scale crystals, *Chem. Eng. Technol.*, 42 (2019) 444–453.
- [29] S. Zhang, H. Qu, Z. Yang, C.E. Fu, Z. Tian, W. Yang, Scale inhibition performance and mechanism of sulfamic/amino acids modified polyaspartic acid against calcium sulfate, *Desalination*, 419 (2017) 152–159.
- [30] H.T. Rahal, A.M. Abdel-Gaber, G.O. Younes, Inhibition of steel corrosion in nitric acid by sulfur containing compounds, *Chem. Eng. Commun.*, 203 (2016) 435–445.
- [31] H.T. Rahal, A.M. Abdel-Gaber, R. Awad, Influence of SnO₂ nanoparticles incorporation on the electrochemical behaviour of a superconductor in sodium sulphate solutions, *Int. J. Electrochem. Sci.*, 12 (2017) 10115–10128.

- [32] H.T. Rahal, A.M. Abdel-Gaber, R. Awad, B.A. Abdel-Naby, Influence of nitrogen immersion and NiO nanoparticles on the electrochemical behavior of (Bi, Pb)-2223 superconductor in sodium sulfate solution, *Anti-Corros. Methods Mater.*, 65 (2018) 430–435.
- [33] M.Y. El Sayed, A.M. Abdel-Gaber, H.T. Rahal, Safranin—a potential corrosion inhibitor for mild steel in acidic media: a combined experimental and theoretical approach, *J. Fail. Anal. Prev.*, 19 (2019) 1174–1180.
- [34] L. Custódio, E. Fernandes, A.L. Escapa, S. López-Avilés, A. Fajardo, R. Aligué, A. Romano, Antioxidant activity and in vitro inhibition of tumor cell growth by leaf extracts from the carob tree (*Ceratonia siliqua*), *Pharm. Biol.*, 47 (2009) 721–728.
- [35] A. Krokou, M. Stylianou, A. Agapiou, Assessing the volatile profile of carob tree (*Ceratonia siliqua* L.), *Environ. Sci. Pollut. Res.*, 26 (2019) 35365–35374.
- [36] NACE (The National Association of Corrosion Engineers) Standard TM0374-95: Laboratory Screening Tests to Determine the Ability of Scale Inhibitors to Prevent the Precipitation of Calcium Sulfate and Calcium Carbonate from Solution (For Oil and Gas Production Systems), NACE (The National Association of Corrosion Engineers), Houston, 1995.
- [37] A. Dugstad, H. Hemmer, M. Seiersten; Effect of steel microstructure on corrosion rate and protective iron carbonate film formation, *Corrosion*, 57 (2001) 369–377.
- [38] M.K. Shahid, Y.G. Choi, The comparative study for scale inhibition on surface of RO membranes in wastewater reclamation: CO₂ purging versus three different antiscalants, *J. Membr. Sci.*, 546 (2018) 61–69.
- [39] T. Chen, A. Neville, M. Yuan, Calcium carbonate scale formation—assessing the initial stages of precipitation and deposition, *J. Pet. Sci. Eng.*, 46 (2005) 185–194.
- [40] H.T. Rahal, A.M. Abdel-Gaber, R. Awad, Corrosion behavior of a superconductor with different SnO₂ nanoparticles in simulated seawater solution, *Chem. Eng. Commun.*, 204 (2017) 348–355.